

1        **Revealing the differences in Collision Cross Section values of small organic**  
2        **molecules acquired by different instrumental designs and prediction models**

3        Lidia Belova<sup>1\*</sup>, Alberto Celma<sup>2</sup>, Glenn Van Haesendonck<sup>3</sup>, Filip Lemièrè<sup>3</sup>, Juan Vicente Sancho<sup>2</sup>,  
4        Adrian Covaci<sup>1</sup>, Alexander L.N. van Nuijs<sup>1</sup>, Lubertus Bijlsma<sup>2\*</sup>

5

6        <sup>1</sup> Toxicological Centre, University of Antwerp, Universiteitsplein 1, 2610 Wilrijk, Belgium

7        <sup>2</sup> Environmental and Public Health Analytical Chemistry, Research Institute for Pesticides and Water,  
8        University Jaume I, Avinguda de Vicent Sos Baynat, 12006 Castelló, Spain

9        <sup>3</sup> Biomolecular & Analytical Mass Spectrometry (BAMS) group, University of Antwerp,  
10       Groenenborgerlaan 171, 2020 Antwerp, Belgium

11

12

13        \*Corresponding authors:

14       Lidia Belova (ORCID: 0000-0001-7147-384X); E-mail: [Lidia.Belova@uantwerpen.be](mailto:Lidia.Belova@uantwerpen.be); Toxicological  
15       Center, University of Antwerp, Universiteitsplein 1, 2610 Wilrijk, Belgium; Phone: +32 3 265 27 02

16       Lubertus Bijlsma (ORCID: 0000-0001-7005-8775); E-mail: [bijlsma@uji.es](mailto:bijlsma@uji.es) ; Environmental and Public  
17       Health Analytical Chemistry, Research Institute for Pesticides and Water, University Jaume I,  
18       Avinguda de Vicent Sos Baynat, 12006 Castelló, Spain

19

20 **ABSTRACT**

21 The number of open access databases containing experimental and predicted collision cross section  
22 (CCS) values is rising and leads to their increased use for compound identification. However, the  
23 reproducibility of reference values with different instrumental designs and the comparison between  
24 predicted and experimental CCS values is still under evaluation.

25 This study compared experimental CCS values of 56 small molecules (Contaminants of Emerging  
26 Concern) acquired by both drift tube (DT) and travelling wave (TW) ion mobility mass spectrometry  
27 (IM-MS). The TWIM-MS included two instrumental designs (Synapt G2 and VION). The experimental  
28  $^{TW}CCS_{N_2}$  values obtained by the TWIM-MS systems showed absolute percent errors (APEs) < 2% in  
29 comparison to experimental DTIMS data, indicating a good correlation between the datasets.  
30 Furthermore,  $^{TW}CCS_{N_2}$  values of  $[M-H]^-$  ions presented the lowest APEs. An influence of the compound  
31 class on APEs was observed.

32 The applicability of prediction models based on artificial neural networks (ANN) and multivariate  
33 adaptive regression splines (MARS), both built using TWIM-MS data, was investigated for the first time  
34 for the prediction of  $^{DT}CCS_{N_2}$  values. For  $[M+H]^+$  and  $[M-H]^-$  ions, the 95<sup>th</sup> percentile confidence intervals  
35 of observed APEs were comparable to values reported for both models indicating a good applicability  
36 for DTIMS predictions.

37 For the prediction of  $^{DT}CCS_{N_2}$  values of  $[M+Na]^+$  ions, the MARS based model provided the best results  
38 with 73.9% of the ions showing APEs below the threshold reported for  $[M+Na]^+$ . Finally,  
39 recommendations for database transfer and applications of prediction models for future DTIMS  
40 studies are made.

41

42 **KEYWORDS**

43 Travelling wave ion mobility separation; drift tube ion mobility separation; compounds of emerging  
44 concern; quality assurance guidelines; CCS comparison; CCS database

45

## 46 1. INTRODUCTION

47 Ion mobility spectrometry (IMS) has demonstrated to be a powerful additional technique for  
48 compound identification within target, suspect and non-target screening studies in various research  
49 fields [1-4]. IMS allows a conformational separation of ions based on their gaseous mobility through a  
50 drift gas (e.g., N<sub>2</sub> or He) under the influence of an electric field. Hence, the hyphenation of IMS with  
51 gas or liquid chromatography (GC or LC) and high resolution mass spectrometry (HRMS) provides an  
52 additional separation dimension [5, 6]. Moreover, the measured drift times can be converted into  
53 collision cross section (CCS) values which describe the rotationally averaged surface of ions for which  
54 collision with the buffer gas occur [7].

55 Drift tube IMS (DTIMS) and travelling wave IMS (TWIMS) are both designed as dispersive techniques,  
56 allowing all ions to pass through for subsequent analysis and are the most commonly applied designs  
57 [8]. DTIMS separates ions in a low uniform electric field (typically 5–100 V/cm). This permits a direct  
58 calculation of CCS values from the measured arrival times ( $t_A$ ; i.e., the time it takes the ion to travel  
59 from the entrance of the drift tube to the detector) without the use of external calibrants provided  
60 that various measurements are conducted applying different electric fields[9, 10]. This is commonly  
61 referred to as the stepped field calibration method. On the contrary, the single field calibration  
62 method allows the calculation of CCS values directly from the  $t_A$  measured at a single electric field  
63 based on a set of calibrant compounds with previously known CCS values [11].

64 TWIMS instruments operate applying both a radio frequency (RF) and a pulsed differential current  
65 (DC) voltage to the ion mobility cell. While the DC voltage ensures the axial movement of ions, the RF  
66 voltage allows radial ion confinement through periodically alternating between positive and negative  
67 polarities [12]. This creates an electric field in the form of a wave whose height and velocity influence  
68 the separation of ions [8]. For TWIMS measurements, a direct calculation of CCS values from the  
69 measured drift times is not possible since the applied electric field is not uniform. However, CCS values  
70 can be calculated based on a set of predefined calibrants whose reference DTIMS derived CCS values  
71 are available. This approach has been described in detail in previous studies [13, 14]. Additionally, it  
72 has been shown that a structural similarity between calibrants and analytes is essential to ensure  
73 reliable CCS calculations [15, 16].

74 Since IMS allows the separation of ions of interest from coeluting matrix components, CCS values are  
75 independent of potential matrix effects or the applied chromatographic conditions[9, 17]. Hence, they  
76 can serve as an additional identification parameter in feature annotation and compound identification  
77 leading to a reduction of false positive identifications [18, 19]. Furthermore, IMS has the potential to  
78 separate isomeric and isobaric compounds. As shown in previous studies, this is especially relevant if  
79 the isomeric compounds have similar retention times (RT) or fragmentation patterns which do not

80 allow their unequivocal identification [19-21]. Additionally, when implemented within data-  
81 independent acquisition (DIA) workflows, IMS facilitates the removal of spectral interferences as these  
82 show different drift times than the compound of interest and its corresponding fragments. This leads  
83 to cleaner mass spectra further improving compound annotation [19, 22].

84 The implementation of IMS in suspect and non-target screening studies on small molecules has been  
85 discussed in detail in previous studies [21, 23-25]. Thereby, CCS values of signals of interest are  
86 matched against CCS values of reference standards, scientific literature or open-source libraries [26-  
87 28], including several online platforms which contain curated CCS datasets from various sources [29-  
88 31]. Moreover, the inclusion of ion mobility data in widely adopted confidence levels for identification  
89 of small molecules in environmental studies, including a cut-off value of 2% for the deviation between  
90 experimental and reference CCS values, has been proposed recently [21].

91 However, the high number of compounds monitored in suspect and non-target screening studies and  
92 the unavailability of reference standards lead to a lack of reference CCS values for many suspects,  
93 currently limiting the use of CCS for compound identification. This data gap can in theory be filled  
94 through the *in-silico* prediction of CCS values. Various prediction tools for different compound classes  
95 are available in the literature [31-36]. These tools are based on experimental CCS values and apply  
96 different predictions models including machine-learning algorithms [31], such as artificial neural  
97 networks (ANN) [36]. Prediction tools have demonstrated good prediction accuracies making them a  
98 valuable addition for suspect and non-target screening studies [37, 38].

99 Despite the high efforts put into CCS database building and the development of prediction models,  
100 CCS values remain an estimated empirical value which is influenced by the instrumental design and  
101 the applied calibration approach. The uncertainty of IMS-MS measurements has been assessed in  
102 detail previously [10, 39]. Several studies have investigated the inter-laboratory and inter-  
103 instrumental reproducibility of CCS measurements [10, 14, 40]. Stow et al. reported a relative standard  
104 deviation (RSD) of 0.29% for stepped-field measurements of  $^{DT}CCS_{N_2}$  values in three different  
105 laboratories of which all applied DTIMS [10]. Hinnenkamp et al. compared CCS values acquired using  
106 TWIMS and DTIMS instruments for a set of 124 compounds and reported absolute errors of < 1% for  
107 66%; between 1-2% for 27% and >2% for 7% of the proton adducts of the investigated compounds  
108 [14].

109 Based on a set of 56 contaminants of emerging concern (CECs) and their metabolites, the present  
110 study aimed to further investigate the reproducibility of CCS values acquired on DTIMS and two  
111 TWIMS instruments applying different calibration approaches and evaluating factors potentially  
112 causing deviations. This work also included the investigation of CCS values for deprotonated ion which  
113 were not present in the above mentioned  $^{DT}CCS_{N_2}$  and  $^{TW}CCS_{N_2}$  comparison [14]. Furthermore, DTIMS

114 derived CCS values were compared with predicted values employing two prediction models built with  
115 TWIMS derived data, namely an ANN based prediction tool and a Multiple Adaptive Regression Splines  
116 (MARS) prediction model previously developed by Bijlsma et al. [36] and by Celma et al. [41],  
117 respectively. Finally, we also aimed to estimate the cut-off values for database transfer from one  
118 instrumental design to another and the applicability of TWIMS-based prediction models for DTIMS  
119 measurements. This study adds to the detailed recommendations for the reporting of experimental  
120 IMS measurements published by Gabelica et al. [9] and it proposes the minimum and most relevant  
121 parameters to be reported for open-access databases of predicted CCS values. These  
122 recommendations will further contribute to a more uniform reporting of IMS data and will allow  
123 potential users to critically review and assess comparability with their own data. The presented results  
124 are expected to serve as a valuable additional guideline for the implementation of IMS in future  
125 studies on small molecule identifications.

126

## 127 **2. Materials and Methods**

### 128 **2.1 Selection of standards**

129 A set of 56 compounds, including five compound classes: triazoles, organophosphate flame retardants  
130 (OPs), plasticizers and metabolites of the latter two, were selected for this comparison study. The  
131 selection of compounds was based on the following considerations: i) inclusion of various compound  
132 classes, incl. metabolites, ii) availability of ions in both ionization polarities, and iii) availability of  
133 reference standards, shared between laboratories. The selected compounds including their name,  
134 abbreviation, molecular formula, structure, SMILES, monoisotopic mass, InChi and InChiKey are  
135 summarized in **Table S1**. The sources from which the reference standards were acquired can be found  
136 in the study from Belova et al. [20].

137

### 138 **2.2 IMS measurements**

#### 139 **2.2.1 DTIMS measurements**

140 The  $^{DT}CCS_{N_2}$  values of the compounds included in this study were previously reported[20] and are  
141 summarized in **Table S1**. In the corresponding publication, a detailed description of the method used  
142 for the acquisition of  $^{DT}CCS_{N_2}$  values can be found. In brief, all  $^{DT}CCS_{N_2}$  values were acquired on an  
143 Agilent 6560 DTIM-QTOF applying the single-field calibration method. For CCS calibration, the ESI low-  
144 concentration tune mix (Agilent Technologies, Santa Clara, USA) was used. The reference  $^{DT}CCS_{N_2}$   
145 values of the tune mix ions were acquired by Stow et al. on a reference DTIMS system [10] and are  
146 summarized in **Table S2** and **Table S3**. Each standard was introduced in the DTIMS-QTOF by direct

147 injection at 1 ng/ $\mu$ L. For each standard, five measurements were conducted. The average  $^{DT}CCS_{N_2}$  value  
148 and (relative) standard deviations are reported (**Table S1**).

149

### 150 **2.2.2 TWIMS measurements (VION)**

151 The first set of  $^{TW}CCS_{N_2}$  values was acquired on a VION IMS-QTOF mass spectrometer (Waters, Milford,  
152 MA, USA), equipped with an electrospray ionization (ESI) interface operating in positive and negative  
153 ionization modes. The ionization source was operated applying the following voltages: capillary  
154 voltage of 0.8 kV; cone voltage 40 V with desolvation temperature set to 550 °C, and the source  
155 temperature to 120 °C. Nitrogen (N<sub>2</sub>) was used as the drying gas and nebulizing gas. The cone gas flow  
156 was 250 L/h and desolvation gas flow of 1000 L/h. MS data were acquired in HDMS<sup>E</sup> mode, over the  
157 range  $m/z$  50-1000, with N<sub>2</sub> as the drift gas, an IMS wave velocity of 250 m s<sup>-1</sup> and wave height ramp  
158 of 20-50 V. Leucine enkephalin ( $m/z$  556.2766 and  $m/z$  554.2620) was used for mass correction in  
159 positive and negative ionization modes, respectively. Two independent scans with different collision  
160 energies were acquired during the run: a collision energy of 6 eV for low energy (LE) and a ramp of 28-  
161 56 eV for high energy (HE). A scan time of 0.3 s was set in both LE and HE functions. Nitrogen ( $\geq$   
162 99.999%) was used as collision-induced dissociation (CID) gas. All data were examined using an in-  
163 house built accurate mass screening workflow within the UNIFI platform (version 1.9.4) from Waters  
164 Corporation. More details about the methodology followed can be found elsewhere [21].

165

### 166 **2.2.3 TWIMS measurements (Synapt G2)**

167 The second set of TWIMS derived  $^{TW}CCS_{N_2}$  values was acquired on a Synapt G2 HD mass spectrometer  
168 (Waters, Milford, MA, USA) equipped with a nano-electrospray ionization source. The ionization  
169 source was operated applying the following voltages: capillary voltage 2.5 kV, extraction cone 5 V;  
170 sample cone 35 V; trap collision energy 4.0 V; transfer collision energy 4.0 V; trap DC bias 35 V. The  
171 wave velocity was set to 1000 m/s at a constant wave height of 40 V. The gas pressures within the  
172 instrument were set as follows: desolvation gas flow 35 L/h (at a temperature of 150 °C); trap gas flow  
173 0.4 mL/min; IMS gas flow 90 mL/min; helium cell gas flow 180 mL/min. For sample infusion, in-house  
174 pulled and gold-coated borosilicate capillaries were used.

175 For the positive ionization mode, calibration compounds proposed by Campuzano et al. were used to  
176 calculate  $^{TW}CCS_{N_2}$  values[42]. For the negative ionization mode, poly-DL-alanine was chosen for CCS  
177 calibration based on the data published by Bush et al. [43]. The molecular formulae, SMILES, CAS  
178 numbers, sources of purchase of the reference standard and reference CCS values of the calibrants  
179 and QA compounds are summarized in **Table S4**.

180 Solutions of the calibration compounds were prepared in water/methanol (50/50; v/v) containing  
181 0.1% formic acid at concentrations between 0.12 ng/ $\mu$ L and 0.61 ng/ $\mu$ L ( $10^{-6}$  M). Solutions of analytes  
182 and quality assurance (QA) compounds were prepared at 1ng/ $\mu$ L in water/acetonitrile (50/50; v/v)  
183 containing 0.1% formic acid. To all infused solutions (both calibrants and analytes) leucine-enkephalin  
184 was spiked prior to infusion at a concentration of 5 ng/ $\mu$ L to be used as a lock-mass for mass calibration  
185 within data analysis. For the measurement of  $^{TW}CCS_{N_2}$  values, all analytes were infused in triplicate.  
186 The instrument was operated using the MassLynx software (version 4.1 SCN 781). After recalibration  
187 based on the added lock-mass of leucine-enkephalin, extracted ion mobilograms for each calibrant  
188 were obtained to allow establishing individual drift time values. The latter were then used to obtain  
189 the calibration curves for positive and negative ionization modes (Figure S1) that enable the  
190 calculation of  $^{TW}CCS_{N_2}$  values. The detailed workflow for  $^{TW}CCS_{N_2}$  calculations has been described in  
191 detail in previous studies [13, 14].

192

### 193 **2.3 Quality assurance (QA) measures**

194 Within each instrumental design used in this study, QA measures were implemented. For DTIMS, the  
195 acquisition of  $^{DT}CCS_{N_2}$  values of nine QA compounds was conducted within each analytical batch. For  
196 these QA compounds reference  $^{DT}CCS_{N_2}$  values acquired on a reference DTIMS system were available  
197 [10]. The QA measures and results of the DTIMS measurements have been described in detail  
198 previously [20].

199 For  $^{TW}CCS_{N_2}$  on the VION system, a set of nine QA compounds included in the System Suitability Test  
200 (SST) mix provided by the manufacturer was used to evaluate the accuracy and performance of the  
201 instrument as well as to ensure the reproducibility of the measurements. The molecular formulae,  
202 SMILES and reference CCS values of the Vion QA compounds are summarized in **Table S5**.

203 Terfenadine, sulfaguanidine, sulfadimethoxine and caffeine were used as QA compounds for  
204 measurements on the Synapt G2 system in positive and sulfaguanidine and sulfadimethoxine in  
205 negative ionization mode, respectively. The selection of QA compounds was based on the compounds  
206 included in the SST mix used for the TWIMS measurements on the Waters VION instrument and aimed  
207 to serve as a QA measure for measurement reproducibility between the two TWIMS set-ups used in  
208 this study. Reference CCS values of the QA compounds were provided by the manufacturer (**Table S4**).

209

### 210 **2.4 CCS predictions**

#### 211 **2.4.1 Artificial Neural Network (ANN) based prediction model**

212 ANN predictions of CCS values were made using Alyuda NeuroIntelligence 2.2 (Cupertino, CA) by  
213 applying a predictor previously developed and optimized [36]. Briefly, eight relevant molecular

214 descriptors of the selected compounds were obtained from an Online Chemical Database  
215 ([www.ochem.eu](http://www.ochem.eu)) [44]. The ANN predictor, trained by means of a database of empirical  $^{TW}CCS_{N_2}$  values  
216 for 205 protonated small molecules, consisted of a neural network structured in three layers with 8-  
217 2-8-1 distribution. The relative error of CCS prediction was within 6% for the 95th percentile of all  
218 values for protonated ions and 8.7% for sodium adducts. Further details on the methodology can be  
219 found elsewhere [36].

220

#### 221 **2.4.2 Multivariate Adaptive Regression Splines (MARS) based prediction model**

222 CCS predictions using Multivariate Adaptive Regression Splines were performed as follows: the  
223 statistical model was trained with empirical  $^{TW}CCS_{N_2}$  values of a total number of 470 protonated ions  
224 and a set of 7 molecular descriptors obtained from the Online Chemical Database ([www.ochem.eu](http://www.ochem.eu))  
225 [44]. The optimized model yielded an accuracy of 4.0% and 5.9% for the 95th percentile of predicted  
226 CCS values of protonated and deprotonated ions, respectively. Moreover, an additional and unique  
227 model was developed for predicting CCS values of sodium adducts obtaining an accuracy of 5.3% (95th  
228 percentile). More details of these prediction models can be found elsewhere [41].

229

### 230 **3. RESULTS AND DISCUSSION**

#### 231 **3.1 Quality control and quality assurance results.**

232 **Figure S2** summarizes the QA approaches implemented in the DTIMS and TWIMS measurements. This  
233 approach used within DTIMS measurements allowed the comparison with reference values obtained  
234 using the same instrumental design leading to low percent errors (PE) (all < 0.2%) [20]. This confirmed  
235 the reproducibility and accuracy of the DTIMS system used in this study.

236 Within the acquisition of  $^{TW}CCS_{N_2}$  values on the TWIMS VION system, the analysis of an SST mixture  
237 containing nine compounds was included (**Table S5**). For these compounds, reference CCS values were  
238 provided by the manufacturer. As it is the case for other reference CCS values used for TWIMS  
239 measurements [42, 43], the provided CCS values were derived from DTIMS based measurements  
240 conducted on a modified Synapt G2 instrument. The VION instrument performance was satisfactory  
241 based on a 2% threshold for the deviation between expected and empirical CCS values.

242 The selection of suitable QA compounds for  $^{TW}CCS_{N_2}$  measurements on the Synapt instrument aimed  
243 to show an overlap with the SST compounds used on the VION system to investigate the  
244 reproducibility between the two TWIMS set-ups. Nevertheless, the QA approaches of both TWIMS  
245 systems must be viewed critically as in both cases experimental  $^{TW}CCS_{N_2}$  values are compared with  
246 DTIMS data. Thus, this approach represents rather a comparison of measurements between the  
247 different TWIMS set-ups than a fully independent QA approach.



248 The results of the Synapt G2 QA measurements are summarized in **Table S6**. Average absolute percent  
249 errors (APEs) of 1.42% and 0.60% were observed for measurements in positive and negative ionization  
250 polarities, respectively. Both values fall within the 2% cut-off for the evaluation of SST measurements  
251 on the VION system and indicate a good reproducibility between the two TWIMS set-ups.  
252 Nevertheless, two QA compounds (sulfaguanidine and caffeine) showed deviations slightly above 2%  
253 in positive mode. These deviations must be interpreted critically as they do not indicate a poor  
254 instrumental performance, but rather a deviation between experimental TWIMS derived CCS values  
255 and the DTIMS based reference values. This will further be investigated in this study. The observed  
256 APEs can also be caused by the low CCS values observed for these compounds ( $CCS < 150 \text{ \AA}^2$ ) whereby  
257 even small deviations in measured  $t_A$  lead to high percent errors.

### 258 **3.2 Selection of reference CCS values for further comparisons**

259 The comparison of experimental DTIMS and TWIMS derived CCS values was based on a set of 56  
260 standards including five compound classes: triazoles, organophosphate flame retardants (OPs),  
261 plasticizers and metabolites of the latter two. Data on proton and sodium adducts, as well as  
262 deprotonated ions were included. In general, the comparison between sets of CCS values is commonly  
263 conducted through reporting the observed (absolute) percent errors [14, 40, 45]. When applying this  
264 approach for the present study, the question about which set of CCS values to use as the reference  
265 set arose. Since none of the datasets was acquired with DTIMS stepped-field calibration, none of the  
266 datasets can be viewed as a calibrant-independent reference. To validate the two prediction models  
267 applied in this study, predicted CCS values have already been compared with the corresponding  
268 experimental TWIMS datasets [36]. Therefore, the use of the  $^{TW}CCS_{N_2}$  dataset as reference would  
269 reproduce this approach and exclude the available  $^{DT}CCS_{N_2}$  values from the comparison. Additionally,  
270 the choice of the reference dataset should allow the comparison of observed deviations between the  
271 different datasets. Therefore,  $^{DT}CCS_{N_2}$  values were used as reference for all calculations included in this  
272 study. Even though these values were acquired using the single-field calibration approach and thus  
273 required calibrants, the influence of the selected calibrants on the reproducibility of measurements  
274 was expected to be lower than for TWIMS calculations [10, 43]. Ultimately, the following equation  
275 was applied for the calculation of percent errors between DTIMS and TWIMS derived or predicted CCS  
276 values:

$$\text{Error [\%]} = \left( \frac{CCS_{TWIMS/pred} - CCS_{DTIMS}}{CCS_{DTIMS}} \right) \cdot 100 \quad (1)$$

277

### 278 **3.3 Comparison of experimental $^{TW}CCS_{N_2}$ and $^{DT}CCS_{N_2}$ values**

279 For the 56 compounds, 108  $^{DT}CCS_{N_2}$  values were included in the DTIMS reference database as several  
280 of the compounds were detected both as proton and sodium adducts and/or in both ionization  
281 polarities. A total of 29  $[M+H]^+$  ions, 46  $[M+Na]^+$  ions and 33  $[M-H]^-$  ions were observed (**Table S1**). The  
282 acquisition of  $^{TW}CCS_{N_2}$  values on the TWIMS VION instrument allowed the detection of a total of 94  
283 ions which corresponded to 50 compounds available for the comparison (**Table S7**). Thus, six  
284 compounds were not detectable on the TWIMS VION set-up which was assumed to be caused by  
285 differences in ionization source parameters and geometries leading to differences in ionization  
286 efficiencies. The 94 detected ions included 22  $[M+H]^+$  ions and 40  $[M+Na]^+$  ions, as well as 32  $[M-H]^-$   
287 ions. Measurements on the Synapt G2 system yielded a total of 97  $^{TW}CCS_{N_2}$  values which corresponded  
288 to 54 compounds detected (**Table S7**). Two compounds, tris(2-ethylhexyl)trimellitate and bisphenol A  
289 bis(diphenyl phosphate), were not detected on the Synapt G2 and VION instruments. Hence, for a  
290 total of 50 compounds, at least one CCS value was available from each of the instrumental set-ups.  
291 Within the 97 ions detected on the Synapt G2 system, 23  $[M+H]^+$ , 41  $[M+Na]^+$  and 33  $[M-H]^-$  ions were  
292 included.

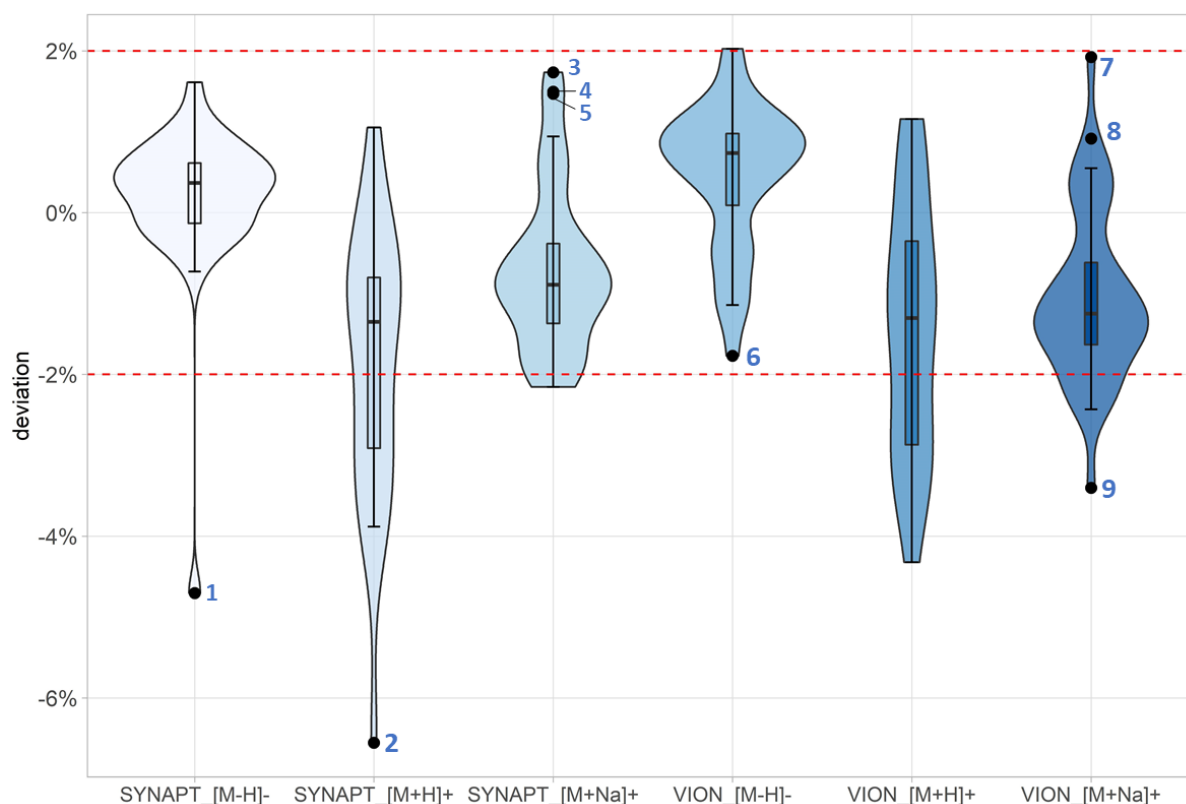
293 As displayed in **Figure S3**, 83% and 82% of all included ions showed APEs < 2% for the comparison of  
294 DTIMS data with the VION and Synapt systems, respectively. For protonated adducts, 64% (VION) and  
295 57% (Synapt) of the observed ions had APEs < 2%. For the sodium adducts, the observed percentages  
296 of ions with APEs < 2% were 83% and 93% for the VION and Synapt systems, respectively.  
297 Deprotonated ions showed the lowest APEs within the comparison between TWIMS and DTIMS  
298 systems. For both VION and Synapt G2 systems, only one  $[M-H]^-$  ion showed an APE > 2% resulting in  
299 97% of  $[M-H]^-$  ions with APEs < 2%.

300 For a more detailed comparison, linear correlations between experimental DTIMS and TWIMS  
301 datasets were investigated. **Figure S4** shows the correlations observed between  $^{DT}CCS_{N_2}$  and  $^{TW}CCS_{N_2}$   
302 values acquired on the VION (**Figure S4A**) and Synapt (**Figure S4B**) systems.

303 For both TWIMS systems, high correlation coefficients ( $R^2$ ) were observed indicating a good linear  
304 correlation between  $^{DT}CCS_{N_2}$  and  $^{TW}CCS_{N_2}$  datasets. However, the  $R^2$  of 0.9889 observed for VION data  
305 was slightly lower than for Synapt data ( $R^2 = 0.9929$ ). Based on a visual inspection of the linear plots,  
306 the higher correlation coefficient observed for Synapt data is assumed to be mainly caused by the  
307 lower deviations from the trendline observed for CCS values of plasticizer metabolites in comparison  
308 with VION derived data. Additionally, interpolated regression lines indicate that  $^{TW}CCS_{N_2}$  datasets can  
309 be correlated to  $^{DT}CCS_{N_2}$  datasets with a slope close to 1 (0.9999 for Vion and 1.0180 for Synapt). This  
310 indicates that deviations between  $^{DT}CCS_{N_2}$  and  $^{TW}CCS_{N_2}$  are negligible, and data can be well compared.  
311 In order to investigate CCS deviations more in detail and distinguish between ionization polarities and

312 ion species, combined violin and box plots of the observed percent errors were created for each  
313 dataset (**Figure 1**).

314



315

316 Figure 1: Combined box and violin plots of the error distributions observed when comparing  $^{DT}CCSN_2$  values with  
317 experimental  $^{TW}CCSN_2$  values *i.e.*, Synapt and Vion acquired in either positive or negative ionization mode. A distinction is  
318 made between proton and sodium adducts. The outliers observed for each dataset are numbered as follows: 1: BTR, 2: 5CI-  
319 BTR, 3: DIDP, 4: DINCH, 5: DIDP, 6: pOH-TPHP, 7: EHDPHP, 8: MiBP, 9: TDCIPP. The full names of the mentioned compounds  
320 can be found in Table S3. A deviation of +/- 2% is indicated with a red dashed line.

321 **Figure 1** shows the combined violin and boxplots of error distributions observed for experimental  
322 TWIMS data acquired in either negative or positive ionization mode. Additionally, bar charts in **Figures**  
323 **S5** and **S6** summarize the percent errors observed for each ion of each individual compound.

324 A threshold of 2% for the use of reference CCS values for compound identification was proposed,  
325 within a recent study [21]. To evaluate the applicability of this threshold for databases acquired with  
326 different instrumental designs, all APEs observed in this study were compared to this cut-off value.

327 For  $[M+H]^+$ , both the Synapt G2 and VION systems show comparable error distributions with mean  
328 values of -1.9% and -1.4% and interquartile ranges (IQR) of 2.1% and 2.5%, respectively. The negative  
329 mean values indicate a clear off-set between DTIMS and TWIMS derived data as most  $^{TW}CCSN_2$  values  
330 of proton adducts were lower than the corresponding  $^{DT}CCSN_2$  values. Except for the VION derived  
331  $^{TW}CCSN_2$  value of tris(1,3-dichloro-2-propyl) phosphate (TDCIPP) with a deviation of -2.84%, all other  
332 deviating  $^{TW}CCSN_2$  values of  $[M+H]^+$  ions belonged either to the group of triazoles or organophosphate  
333 flame retardants (and metabolites) carrying at least two phenyl moieties. Triazoles represent the class

334 with the lowest  $m/z$  values ( $m/z$  118 – 154) investigated in the study. Low  $m/z$  values result in lower  
335 CCS values for which even small absolute deviations can lead to high percentual errors. As it was  
336 previously observed for diphenyl phthalate (DPP) [20], aromatic substitutes are assumed to lead to  
337 more compact ions resulting in lower  $^{DT}CCS_{N_2}$  values. The observed deviations of TWIMS data lead to  
338 the assumption that this effect has a higher influence within DTIMS measurements, indicating differing  
339 molecular conformations of the described compounds between TWIMS and DTIMS systems.

340 Interestingly, the error distributions observed for  $[M+Na]^+$  show a smaller spread in comparison to the  
341 protonated ions. The deviations calculated for  $[M+Na]^+$  showed mean values of -0.7% and -1.0% and  
342 IQRs of 1.0% and 1.0% for the Synapt and VION systems, respectively. A study by Hinnenkamp et al.  
343 reported slightly higher percent errors for sodium adducts in comparison to protonated ions: 87% of  
344 the included  $[M+Na]^+$  ions showed APEs < 2% while this percentage was 93% for  $[M+H]^+$  [14]. This was  
345 assumed to be caused by the fact that sodium adducts were not included in the ions used as calibrants  
346 for TWIMS measurements. However, these observations were not reproduced in this study which  
347 might be caused by different compound classes or sample sizes included in the two studies. Again, a  
348 negative off-set between  $^{TW}CCS_{N_2}$  and  $^{DT}CCS_{N_2}$  values was observed, as most  $^{TW}CCS_{N_2}$  values of  $[M+Na]^+$   
349 ions were lower than the corresponding DTIMS values (**Figures S4** and **S5**). From the VION derived  
350  $^{TW}CCS_{N_2}$  values of  $[M+Na]^+$  ions, for seven values an APE > 2% was observed. Again, four of the seven  
351 values belonged to organophosphate flame retardants (OPs) and their metabolites carrying phenyl  
352 moieties. From the Synapt derived  $^{TW}CCS_{N_2}$  values of  $[M+Na]^+$  ions, three values showed a APE > 2%.  
353 All of these deviating values overlapped with the deviating VION derived values and included two OPs  
354 carrying phenyl moieties (triphenyl phosphate and diphenylcresyl phosphate). Except for mono-(3-  
355 carboxypropyl) phthalate (PE of -2.2%), all remaining deviating  $^{TW}CCS_{N_2}$  values of  $[M+Na]^+$  ions belong  
356 to the group of halogenated OPs and metabolites. Here, an influence of the applied calibrants is  
357 assumed. While the calibrants used for DTIMS measurements included several halogenated  
358 compounds (Tables **S2** and **S3**), this was not the case for neither the Synapt nor the VION calibrations  
359 possibly leading to the observed high deviations for halogenated compounds. The latter was  
360 confirmed by the fact that the  $^{TW}CCS_{N_2}$  values of the  $[M+H]^+$  ion of 5-chlorobenzotriazole (5Cl-BTR)  
361 showed the highest deviation of all  $[M+H]^+$  ions for both the VION and Synapt systems (outlier nr. 2 in  
362 **Figure 1**). However, further investigations are needed to confirm these effects for larger sample sizes  
363 and wider  $m/z$  ranges.

364 Within the Synapt dataset of  $[M+Na]^+$  ions, three outliers (nr. 3-5 in **Figure 1**) with higher  $^{TW}CCS_{N_2}$   
365 values in comparison to the corresponding  $^{DT}CCS_{N_2}$  values were identified. These values derived from  
366 diisodecyl phthalate (DIDP), diisononyl phthalate (DINP) and diisononyl cyclohexane 1,2-dicarboxylic  
367 acid (DINCH). For two of these compounds (DIDP and DINCH), the  $^{DT}CCS_{N_2}$  values of sodium adducts

368 were lower than the corresponding values of protonated adducts which was in contrast to the trend  
369 observed for most other compounds included in the  $^{DT}CCS_{N_2}$  database[20]. This observation was not  
370 reproduced for the Synapt derived  $^{TW}CCS_{N_2}$  values leading to the assumption of different ion  
371 conformations being observed between the TWIMS and DTIMS systems due to slight differences in  
372 ionization processes. Alternatively, the fact that the used DIDP and DINCH standards represented  
373 mixtures of isomers could also lead to the described observations.

374 During the comparison of datasets acquired in positive ionization polarity, an unexpectedly high error  
375 (15.31%) was observed for the proton adduct of bis(1,3-dichloro-2-propyl) phosphate (BDCIPP). A  
376 close reinvestigation of the DTIMS raw data indicated that the high  $^{DT}CCS_{N_2}$  value was caused by an  
377 impurity of tris(1,3-dichloro-2-propyl) phosphate (TDCIPP) in the BDCIPP standard from which latter  
378 was formed through post drift tube fragmentation. This led to a signal for BDCIPP which showed the  
379 same drift time as tris(1,3-dichloro-2-propyl) phosphate leading to the high CCS value. Within the plots  
380 of  $m/z$  versus CCS values which were created from the DTIMS dataset[20], the incorrectly assigned  
381 CCS values had not shown a clear deviation from the observed trendlines. Thus, the incorrect  
382 assignment could not be identified prior to the comparison conducted in this study. The BDCIPP  
383 standard was reanalyzed using the same workflow[20]. These measurements lead to a  $^{DT}CCS_{N_2}$  value  
384  $157.35 \text{ \AA}^2$  and a lower observed deviation (-1.5 %). This value was used for all comparisons described  
385 above and was added to the previously published DTIMS database to correct the incorrect assignment.

386 For the dataset acquired in negative ionization polarity, the observed deviations show a lower spread  
387 compared to the positive ionization mode. This reflects in the low IQRs of 0.7% and 0.9% for Synapt  
388 and VION datasets, respectively. Within the Synapt G2 dataset, all APEs of negatively charged ions  
389 were < 2%, except for the outlier indicated in **Figure 1** (outlier nr. 1,  $[M-H]^-$  ion of benzotriazole). For  
390 the VION dataset, one out of 32 CCS values of  $[M-H]^-$  ions showed an APE of > 2% ( $[M-H]^-$  ion of 2,4-  
391 di-(2-ethylhexyl) trimellitate). These observations indicate a high reproducibility of CCS values of  $[M-  
392 H]^-$  ions between different instrumental set-ups. The observed high reproducibility might be due to  
393 the fact that OPs and their metabolites (for which high deviations were observed in positive ionization  
394 polarity) were not included, since these compounds were not detected in negative ionization polarity.  
395 Additionally, an opposite trend in comparison to data obtained in positive ionization polarity was  
396 observed: both datasets showed a positive median error indicating a positive off-set between TWIMS  
397 and DTIMS data. The included compound classes which differed between the datasets might have an  
398 influence on these effects.

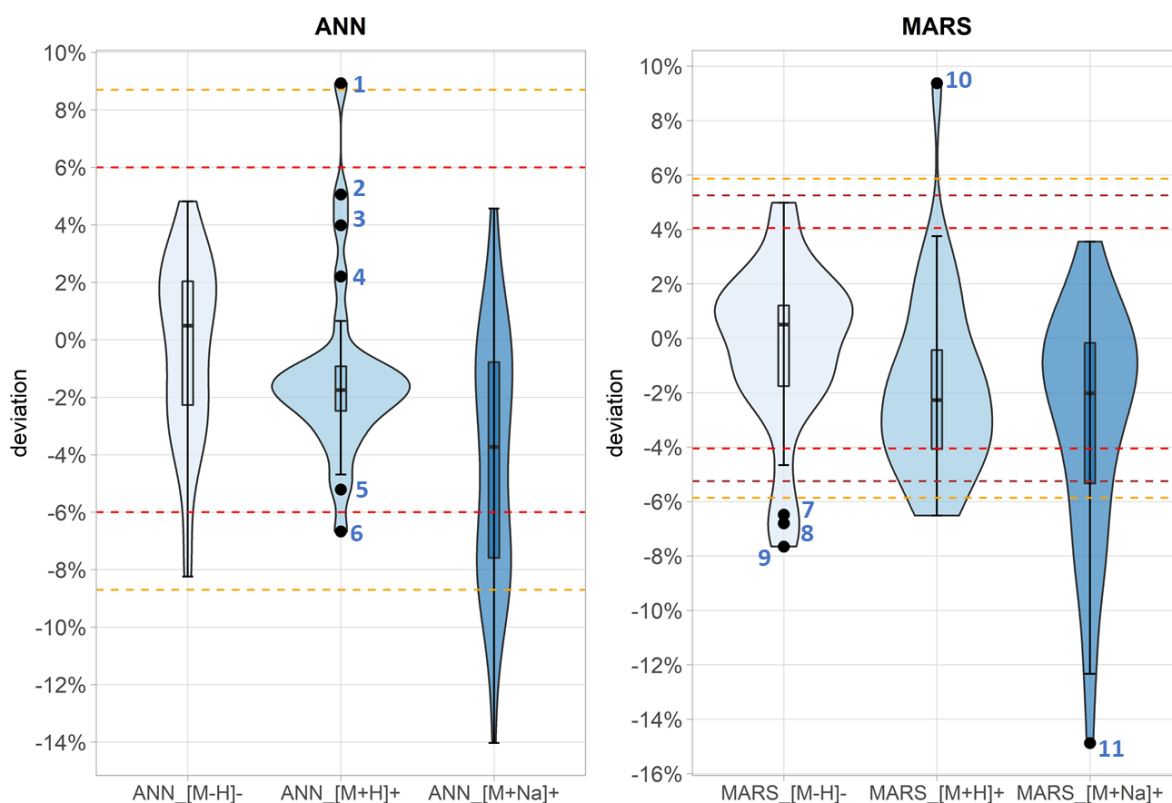
399 Good correlations were observed between DTIMS and TWIMS derived CCS values. Nevertheless, a few  
400 compounds showed high deviations of up to -4.3% and -6.6%. Several potential factors which might

401 cause the high deviations could be identified and must be considered when interpreting the quality  
402 and reliability of the presented dataset. Firstly, an influence of the compound class can be assumed  
403 as most of the highly deviating values derived from a particular class (OPs and their metabolites  
404 carrying at least two phenyl substituents). These effects might be traced back to differences in ion  
405 conformations between DTIMS and TWIMS systems for certain classes. Secondly, an effect of the  
406 applied calibration approach on CCS deviations is considered possible. Several previous studies have  
407 characterized the influence of the calibrants applied for TWIMS measurements and addressed the  
408 advantage of a match in compound class and charge state between calibrants and analytes. However,  
409 most of these studies focused on proteomic and lipidomic applications, which means that only a  
410 limited amount of studies including small molecules applications can be found [15, 16, 46]. Recently,  
411 a study assessed the influence of different calibration approaches on TWIMS measurements of  
412 steroids evaluating and comparing the observed bias. Additionally, a new set of reference DTIMS  
413 derived CCS values for TWIMS calibration was proposed whose implementation improved the  
414 reproducibility of CCS measurements on different instrumental set-ups [47]. These observations  
415 highlight the need of similar evaluations of different calibration approaches for the analysis of CECs  
416 and a potential implementation of the newly proposed sets of reference CCS values. A critical manual  
417 evaluation of the calibration approaches applied for the compilation of TWIMS derived databases thus  
418 remains crucial before database implementation for different instrumental designs and/or calibration  
419 approaches. Lastly, the described limitations confirm that CCS values represent empirical  
420 measurements which are influenced by several factors and do not allow the establishment of a “true  
421 CCS value”. It is recommended to assess potential deviations based on a subset of reference standards  
422 of the class of interest prior to applying a database acquired with a different instrumental design.  
423 Subsequently, the cut-off value of 2% which has been proposed previously[21] might need to be  
424 adjusted for databases deriving from different instrumental designs or different calibration  
425 approaches.

### 426 **3.4 Comparison of predicted CCS and experimental <sup>DT</sup>CCS<sub>N2</sub> values**

427 The experimental <sup>DT</sup>CCS<sub>N2</sub> values were compared with predicted datasets which derived from two  
428 different prediction models, namely an ANN and a MARS based model [36, 41]. Both models were  
429 built using experimental TWIMS derived CCS values. To the best of our knowledge, this is the first  
430 study investigating the capabilities of these models in predicting CCS values for DTIMS measurements.  
431 During the development of the ANN based prediction model, an APE < 6% was observed for 95% of  
432 the protonated ions when comparing predicted with experimental <sup>TW</sup>CCS<sub>N2</sub> values. To be able to  
433 compare these observations, the same threshold (6%) was applied to assess the deviations of ANN  
434 based predicted CCS values (further referred to as CCS<sub>ANN</sub>) of [M+H]<sup>+</sup> ions presented here. A 6%

435 threshold was also used to assess deviations of  $[M-H]^-$  ions, even though it must be noted that the  
436 ANN based model was built using  $[M+H]^+$  data, but not evaluated for  $[M-H]^-$  ions within its  
437 development. For  $[M+Na]^+$  ions, an APE of 8.7% was reported for the 95<sup>th</sup> percentile confidence  
438 interval [36]. This higher value is caused by the fact that the ANN based prediction model has been  
439 developed without the inclusion of  $[M+Na]^+$  ions in the training, validation and blind datasets [36]. On  
440 the contrary to the  $[M-H]^-$  ions,  $[M+Na]^+$  data has been evaluated within its development. Hence, a  
441 threshold of 8.7% was applied for  $[M+Na]^+$  ions as higher APEs can be assumed for this ion species.  
442 **Figure 2** shows the combined violin and boxplots of the error distributions observed for predicted CCS  
443 values differentiating between prediction models and ion species. For the linear correlation between  
444  $^{DT}CCS_{N_2}$  and  $CCS_{ANN}$  values, a correlation coefficient of  $R^2 = 0.9305$  and a slope of 0.9753 were observed  
445 (see **Figure S7A**). For  $[M+H]^+$  ions, the ANN based model showed a median APE of -1.8% and an IQR of  
446 1.6%. Due to the small IQR (in comparison to other ion species) which influences the upper and lower  
447 fence (defined as the  $Q_3/Q_1 \pm 1.5 \times IQR$ ), several outliers were observed (see **Figure 2**). Similar to the  
448 comparison of experimental  $^{DT}CCS_{N_2}$  and  $^{TW}CCS_{N_2}$  values, all observed outliers belonged to either OPs  
449 (and metabolites) with at least two aromatic moieties or low-mass (halogenated) triazoles.  
450 Nevertheless, most of the observed outliers fall within the threshold of  $\pm 6\%$  resulting in 93.1% of the  
451  $CCS_{ANN}$  values showing an APE  $< 6\%$ . Comparable results were obtained for  $CCS_{ANN}$  values of  $[M-H]^-$  ions  
452 of which 93.9% showed APEs  $< 6\%$  with only two values exceeding this threshold ( $CCS_{ANN}$  of mono(2-  
453 ethylhexyl) terephthalate and mono(2-ethyl-5-hydroxyhexyl) terephthalate). Therefore, for  $[M-H]^-$   
454 and  $[M+H]^+$ , it can be concluded that the ANN based prediction model can successfully be applied for  
455 DTIMS measurements of small molecules structurally similar to the compound classes investigated  
456 here. Again, the deviations observed for some classes point out the necessity of evaluating the  
457 applicability of the model based on a subset of reference standards.  
458  $CCS_{ANN}$  values of  $[M+Na]^+$  ions show the highest APE with a median value of -3.7% and an IQR of 6.8%.  
459 From the 46  $[M+Na]^+$  ions included in the comparison, 80.4 % showed an APE below the applied  
460 threshold ( $< 8.7\%$ ). Similar to the conclusions made within the development of the ANN based model,  
461 a higher cut-off value is recommended when applying the model for the prediction of  $[M+Na]^+$  ions  
462 within DTIMS measurements (see below).



463  
 464 **Figure 2:** Combined violin and boxplots of the error distributions observed when comparing  $^{DT}CCS_{N_2}$  values with predicted  
 465 CCS values deriving from Artificial Neural Network (ANN) and Multivariate Adaptive Regression Splines (MARS) based models.  
 466 For data in positive ionization polarity, a distinction between proton and sodium adducts is made. The outliers observed for  
 467 each dataset are numbered as follows: 1: Fyroxflex BDP, 2: 5OH-EHDPPH, 3: Fyroxflex RDP, 4: TOTP, 5: 4OH-PhP, 6: 5Cl-BTR, 7:  
 468 2,4-DEHTM, 8: MEHTP, 9: 5OH-MEHTP, 10: Fyroxflex BDP, 11: TOTM. The full names of the mentioned compounds can be  
 469 found in Table S3. The thresholds applied for the comparisons are indicated with dashed lines. These thresholds are based  
 470 considering the 95<sup>th</sup> confidence interval of each model. For the ANN based model, thresholds of 6% ([M+H]<sup>+</sup> and [M-H]<sup>-</sup> ions;  
 471 red dashed line) and 8.7% ([M+Na]<sup>+</sup>; orange dashed line) were applied. MARS based data was compared based on thresholds  
 472 of 4.1% (red dashed line), 5.9% (orange dashed line) and 5.3% (brown dashed line) for [M+H]<sup>+</sup>, [M+Na]<sup>+</sup> and [M-H]<sup>-</sup> ions,  
 473 respectively.

474 In contrast to the ANN based prediction model, the MARS based model was validated for all ion species  
 475 included here (*i.e.*, [M+H]<sup>+</sup>, [M+Na]<sup>+</sup> and [M-H]<sup>-</sup> ions). This allowed the reporting of APEs observed for  
 476 the 95<sup>th</sup> percentile of the datapoints for each ion species separately [41]. In detail, these APEs  
 477 corresponded to 4.1%, 5.9% and 5.3% for [M+H]<sup>+</sup>, [M-H]<sup>-</sup> and [M+Na]<sup>+</sup> ions, respectively [41], which  
 478 will be used as thresholds to access the deviations presented in this study.

479 From the CCS values predicted for [M+H]<sup>+</sup> ions applying the MARS based model (further referred to as  
 480  $CCS_{MARS}$ ), 71.9% showed an APE < 4.0%. This corresponds to 9 out of 32  $CCS_{MARS}$  values for [M+H]<sup>+</sup> ions  
 481 showing an APE above the applied threshold. Two of these deviating  $CCS_{MARS}$  values were also  
 482 observed as deviating  $CCS_{ANN}$  values, namely BDP ( $CCS_{MARS}$  with a deviation of 9.38%) and 5Cl-BTR  
 483 ( $CCS_{MARS}$  with a deviation of -6.52%). Additionally, the  $CCS_{MARS}$  values of DIDP, DINP and DINCH showed  
 484 APEs > 4.0%. The same assumptions as described about the causes of these deviations can be applied  
 485 here.



486 For the  $[M+Na]^+$  ions, 73.9% of which showed an APE <5.3%, a median deviation of -2.3% and an IQR  
 487 of 5.2% were observed. This indicates higher (i.e., closer to zero) median values and a smaller IQR than  
 488 observed for  $CCS_{ANN}$  values of sodium adducts. Within the development of the MARS based model, a  
 489 separate model was developed for the prediction of CCS values of  $[M+Na]^+$  ions. Thereby,  
 490 experimental values of  $[M+Na]^+$  adducts were included in the training dataset to account for the  
 491 higher volume and particularities derived from the allocation of the sodium ion within the molecular  
 492 structure influencing the shape and size of ions [41]. The lower APEs observed for  $CCS_{MARS}$  values of  
 493 sodium adducts confirm the added value of the described approach indicating that the MARS based  
 494 model is more suitable for a reliable prediction of CCS values for this ion species. Nevertheless, the  
 495 APEs reported here still show higher deviations than observed for the comparison with experimental  
 496 TWIMS based values [41] indicating that additional factors influence the accuracy of the prediction.  
 497 For  $CCS_{MARS}$  values of  $[M-H]^-$  ions, a median deviation of 0.5% and an IQR of 3.0% were observed. 90.0%  
 498 of the  $CCS_{MARS}$  values of  $[M-H]^-$  ions showed an APE < 5.9%. This corresponds to 3 out of 30  $CCS_{MARS}$   
 499 values with an APE >5.9% which are indicated as outliers in **Figure 2**. Two of the corresponding  
 500 compounds (MEHTP and 5-HO-MEHTP) had also shown high deviations within their ANN based  
 501 predicted values. Based on the low number of terephthalates and metabolites included in the dataset,  
 502 it cannot be stated whether particular structural characteristics or other factors cause the observed  
 503 high deviations. The same applies to the high deviation observed for the  $CCS_{MARS}$  value of the  $[M-H]^-$   
 504 ion of 2,4-DEHTM (-6.48%).

505

506 Table 1: The 95<sup>th</sup> percentiles observed for the absolute percent errors (APEs) between experimental  $^{DT}CCS_{N_2}$  values and  
 507 predicted CCS values. The latter were predicted applying Artificial Neural Network (ANN) and Multivariate Adaptive  
 508 Regression Splines (MARS) based models.

Ion species	95 <sup>th</sup> percentile of observed APEs	
	ANN	MARS
$[M+H]^+$	6.08%	6.38%
$[M+Na]^+$	10.29%	11.13%
$[M-H]^-$	5.70%	6.66%

509

510 The percentages of ions showing an APE below the applied thresholds are summarized in **Table S9**.  
 511 Additionally, the 95<sup>th</sup> percentiles of the absolute percent errors observed for each ion species were  
 512 calculated (**Table 1**). This aimed at estimating thresholds recommended for future applications of the  
 513 ANN and MARS based models for DTIMS measurements. From the observed 95<sup>th</sup> percentiles the  
 514 conclusion might be drawn that the ANN based model provides better results for DTIMS predictions,  
 515 as all reported values are lower in comparison to the MARS based model. However, in contrast to the  
 516 95<sup>th</sup> percentiles which were reported within the development of the prediction models[36, 41], the  
 517 values reported in this study are based on a smaller sample size. Thus, after grouping the observed

518 APEs by size, the reported 95<sup>th</sup> percentile is strongly influenced by the data points determining the  
 519 95% cut-off. Due to the small percentage range and sample size investigated, even slight deviations of  
 520 these values towards higher APEs can have strong effects on the calculated percentiles. Especially for  
 521 [M+Na]<sup>+</sup> ions, this approach does not reflect the added advantages of the MARS based model  
 522 described above, thus not allowing the direct use of the 95<sup>th</sup> percentiles as proposed thresholds.  
 523 Nevertheless, the 95<sup>th</sup> percentiles reported reflect deviations between experimental <sup>DT</sup>CCS<sub>N2</sub> values  
 524 and predicted data which are comparable to the observations reported within the development of the  
 525 prediction models, thus indicating their applicability for DTIMS measurements. It is recommended to  
 526 use the reported 95<sup>th</sup> percentiles in combination with an assessment of possible deviations for the  
 527 compound class of interest to estimate applicable thresholds. The MARS based model is  
 528 recommended for the prediction of [M+Na]<sup>+</sup> ions[41].  
 529 The described considerations indicate the necessity of a critical expert evaluation of the applicability  
 530 of a prediction model prior to its implementation. The discussion presented here also points out that  
 531 the various factors influencing both the experimental acquisition and prediction of CCS values do not  
 532 allow, at this moment, an unsupervised implementation of prediction models and databases acquired  
 533 on different instrumental set-ups.

534

### 535 **3.5 Recommendation of parameters to be reported for CCS prediction models**

536 The acquisition of CCS values represents a measurement of empirical values rather than an absolute  
 537 and constant physical property. Therefore, a detailed reporting of experimental settings, as well as  
 538 applied QA measures is crucial to estimate the influence of these parameters on IMS-MS  
 539 measurements and their reproducibility using other instrumental designs. Parameters recommended  
 540 to be reported for experimental CCS values have been discussed in detail by Gabelica *et al.* [9] and  
 541 include mainly mobility device hardware parameters, used drift gas and calibrants or QC compounds.  
 542 The observed deviations between <sup>DT</sup>CCS<sub>N2</sub> and <sup>TW</sup>CCS<sub>N2</sub> values described for some of the compound  
 543 classes investigated in the presented study confirm the necessity of a unified reporting of  
 544 experimental parameters to trace back possible causes for such findings. Adding to these  
 545 recommendations, this study proposes a set of parameters recommended to be reported for CCS  
 546 prediction models in order to highlight their usefulness for other instrumental designs (**Table 2**).

547

548 Table 2: Recommended parameters for the reporting of CCS prediction models.

Parameter	Recommended information to report
General	General aim of the development. For which compound classes is the model being developed? Which experimental datasets will be used for the development?

Prediction model	Characteristics of applied prediction model; settings and descriptors used for training of the model
Training set	Detailed information on the identity of compounds used for training of the model; ion species included in the training set; detailed description of experimental parameters used for the acquisition of experimental CCS values used for training of the model
Validation results	Description of results obtained after validating the developed model; description of validation dataset and detailed reporting of results for each ion species. Which thresholds should be applied in future applications of the prediction model?
Inter-lab validation	Evaluation of prediction performance of the model for the particular instrument in use. Study of accuracy of prediction for a small set of molecules to support the decisions on suspect substances.

549

#### 550 4. CONCLUSIONS

551 A dataset containing 106 DTIMS derived  $^{DT}CCS_{N_2}$  values including  $[M+H]^+$ ,  $[M+Na]^+$  and  $[M-H]^-$  ions was  
552 compared with both experimental (TWIMS derived)  $^{TW}CCS_{N_2}$  values and predicted CCS values.  $^{TW}CCS_{N_2}$   
553 values were acquired on a VION and Synapt G2 system showing absolute errors < 2% for 83% and 82%  
554 of the values, respectively, indicating a good reproducibility between different instrumental designs.  
555 Moreover, good linear correlations were observed for both systems resulting in correlation  
556 coefficients of  $R^2 = 0.9889$  (VION) and  $R^2 = 0.9929$  (Synapt). Nevertheless, deviations of up to -6.55%  
557 were observed for a few compounds belonging to particular chemical classes of compounds,  
558 Additionally, the applied calibration approaches could not be excluded as a potential cause for the  
559 observed deviations. These findings point out that potential biases of experimental databases built on  
560 data acquired by a different instrumental set-up, need to be evaluated prior to its implementation.  
561 With regards to CCS prediction models, the 95<sup>th</sup> percentiles of deviations reported for  $[M+H]^+$  and  $[M-$   
562  $H]^-$  ions between experimental  $^{DT}CCS_{N_2}$  values and predicted data were comparable to the values  
563 reported within the development of the ANN and MARS based models, indicating their applicability  
564 for DTIMS measurements. These percentiles can be used to establish thresholds to be applied in future  
565 DTIMS based studies. However, different parameters such as the aim and compound class for which  
566 the model is developed should be considered prior to its applications.

567

#### 568 5. ACKNOWLEDGMENTS

569 L. Belova acknowledges funding through a Research Foundation Flanders (FWO) fellowship  
570 (11G1821N). L. Bijlsma acknowledges his fellowship funded by "la Caixa" Foundation. The project that  
571 gave rise to these results also received the support of a fellowship from "la Caixa" Foundation (ID 10  
572 0 010434). The fellowship code is LCF/BQ/PR21/11840012. Jesse Sterckx is acknowledged for helping

573 with the measurements on the Synapt G2 system. This work received financial support also from the  
574 University Jaume I (UJI-B2020-19). The graphical abstract was created with BioRender.com, license no  
575 2641-5211.

## 576 6. REFERENCES

- 577 [1] L. Mullin, K. Jobst, R.A. DiLorenzo, R. Plumb, E.J. Reiner, L.W.Y. Yeung, I.E. Jogsten, Liquid  
578 chromatography-ion mobility-high resolution mass spectrometry for analysis of pollutants in indoor  
579 dust: Identification and predictive capabilities, *Anal Chim Acta* 1125 (2020) 29-40.
- 580 [2] A.D. George, M.C.L. Gay, M.E. Wlodek, R.D. Trengove, K. Murray, D.T. Geddes, Untargeted  
581 lipidomics using liquid chromatography-ion mobility-mass spectrometry reveals novel  
582 triacylglycerides in human milk, *Sci Rep* 10(1) (2020) 9255.
- 583 [3] L. Lacalle-Bergeron, T. Portoles, F.J. Lopez, J.V. Sancho, C. Ortega-Azorin, E.M. Asensio, O. Coltell,  
584 D. Corella, Ultra-Performance Liquid Chromatography-Ion Mobility Separation-Quadruple Time-of-  
585 Flight MS (UHPLC-IMS-QTOF MS) Metabolomics for Short-Term Biomarker Discovery of Orange  
586 Intake: A Randomized, Controlled Crossover Study, *Nutrients* 12(7) (2020).
- 587 [4] T.J. Causon, V. Ivanova-Petropulos, D. Petrusheva, E. Bogeva, S. Hann, Fingerprinting of  
588 traditionally produced red wines using liquid chromatography combined with drift tube ion mobility-  
589 mass spectrometry, *Anal Chim Acta* 1052 (2019) 179-189.
- 590 [5] J. Hollender, E.L. Schymanski, H.P. Singer, P.L. Ferguson, Nontarget Screening with High  
591 Resolution Mass Spectrometry in the Environment: Ready to Go?, *Environ Sci Technol* 51(20) (2017)  
592 11505-11512.
- 593 [6] M. Pourchet, L. Debrauwer, J. Klanova, E.J. Price, A. Covaci, N. Caballero-Casero, H. Oberacher, M.  
594 Lamoree, A. Damont, F. Fenaille, J. Vlaanderen, J. Meijer, M. Krauss, D. Sarigiannis, R. Barouki, B. Le  
595 Bizec, J.P. Antignac, Suspect and non-targeted screening of chemicals of emerging concern for  
596 human biomonitoring, environmental health studies and support to risk assessment: From promises  
597 to challenges and harmonisation issues, *Environ Int* 139 (2020) 105545.
- 598 [7] J.W. Lee, Basics of Ion Mobility Mass Spectrometry, *Mass Spectrometry Letters* 8(4) (2017) 79-89.
- 599 [8] V. D'Atri, T. Causon, O. Hernandez-Alba, A. Mutabazi, J.L. Veuthey, S. Cianferani, D. Guillaume,  
600 Adding a new separation dimension to MS and LC-MS: What is the utility of ion mobility  
601 spectrometry?, *J Sep Sci* 41(1) (2018) 20-67.
- 602 [9] V. Gabelica, A.A. Shvartsburg, C. Afonso, P. Barran, J.L.P. Benesch, C. Bleiholder, M.T. Bowers, A.  
603 Bilbao, M.F. Bush, J.L. Campbell, I.D.G. Campuzano, T. Causon, B.H. Clowers, C.S. Creaser, E. De  
604 Pauw, J. Far, F. Fernandez-Lima, J.C. Fjeldsted, K. Giles, M. Groessl, C.J. Hogan, Jr., S. Hann, H.I. Kim,  
605 R.T. Kurulugama, J.C. May, J.A. McLean, K. Pagel, K. Richardson, M.E. Ridgeway, F. Rosu, F. Sobott, K.  
606 Thalassinos, S.J. Valentine, T. Wyttenbach, Recommendations for reporting ion mobility Mass  
607 Spectrometry measurements, *Mass Spectrom Rev* 38(3) (2019) 291-320.
- 608 [10] S.M. Stow, T.J. Causon, X. Zheng, R.T. Kurulugama, T. Mairinger, J.C. May, E.E. Rennie, E.S.  
609 Baker, R.D. Smith, J.A. McLean, S. Hann, J.C. Fjeldsted, An Interlaboratory Evaluation of Drift Tube  
610 Ion Mobility-Mass Spectrometry Collision Cross Section Measurements, *Anal Chem* 89(17) (2017)  
611 9048-9055.
- 612 [11] R.T. Kurulugama, E. Darland, F. Kuhlmann, G. Stafford, J. Fjeldsted, Evaluation of drift gas  
613 selection in complex sample analyses using a high performance drift tube ion mobility-QTOF mass  
614 spectrometer, *Analyst* 140(20) (2015) 6834-44.
- 615 [12] K. Giles, S.D. Pringle, K.R. Worthington, D. Little, J.L. Wildgoose, R.H. Bateman, Applications of a  
616 travelling wave-based radio-frequency-only stacked ring ion guide, *Rapid Commun Mass Spectrom*  
617 18(20) (2004) 2401-14.
- 618 [13] B.T. Ruotolo, J.L. Benesch, A.M. Sandercock, S.-J. Hyung, C.V. Robinson, Ion mobility-mass  
619 spectrometry analysis of large protein complexes, *Nat Protoc* 3(7) (2008) 1139-1152.

620 [14] V. Hinnenkamp, J. Klein, S.W. Meckelmann, P. Balsaa, T.C. Schmidt, O.J. Schmitz, Comparison of  
621 CCS Values Determined by Traveling Wave Ion Mobility Mass Spectrometry and Drift Tube Ion  
622 Mobility Mass Spectrometry, *Anal Chem* 90(20) (2018) 12042-12050.

623 [15] A.S. Gelb, R.E. Jarratt, Y. Huang, E.D. Dodds, A study of calibrant selection in measurement of  
624 carbohydrate and peptide ion-neutral collision cross sections by traveling wave ion mobility  
625 spectrometry, *Anal Chem* 86(22) (2014) 11396-11402.

626 [16] M.F. Bush, Z. Hall, K. Giles, J. Hoyes, C.V. Robinson, B.T. Ruotolo, Collision cross sections of  
627 proteins and their complexes: a calibration framework and database for gas-phase structural  
628 biology, *Anal Chem* 82(22) (2010) 9557-9565.

629 [17] V. Gabelica, E. Marklund, Fundamentals of ion mobility spectrometry, *Curr Opin Chem Biol* 42  
630 (2018) 51-59.

631 [18] T.O. Metz, E.S. Baker, E.L. Schymanski, R.S. Renslow, D.G. Thomas, T.J. Causon, I.K. Webb, S.  
632 Hann, R.D. Smith, J.G. Teeguarden, Integrating ion mobility spectrometry into mass spectrometry-  
633 based exposome measurements: what can it add and how far can it go?, *Bioanalysis* 9(1) (2017) 81-  
634 98.

635 [19] A. Celma, L. Ahrens, P. Gago-Ferrero, F. Hernandez, F. Lopez, J. Lundqvist, E. Pitarch, J.V. Sancho,  
636 K. Wiberg, L. Bijlsma, The relevant role of ion mobility separation in LC-HRMS based screening  
637 strategies for contaminants of emerging concern in the aquatic environment, *Chemosphere* 280  
638 (2021) 130799.

639 [20] L. Belova, N. Caballero-Casero, A.L.N. van Nuijs, A. Covaci, Ion Mobility-High-Resolution Mass  
640 Spectrometry (IM-HRMS) for the Analysis of Contaminants of Emerging Concern (CECs): Database  
641 Compilation and Application to Urine Samples, *Anal Chem* 93(16) (2021) 6428-6436.

642 [21] A. Celma, J.V. Sancho, E.L. Schymanski, D. Fabregat-Safont, M. Ibanez, J. Goshawk, G.  
643 Barknowitz, F. Hernandez, L. Bijlsma, Improving Target and Suspect Screening High-Resolution Mass  
644 Spectrometry Workflows in Environmental Analysis by Ion Mobility Separation, *Environ Sci Technol*  
645 54(23) (2020) 15120-15131.

646 [22] L. Bijlsma, R. Bade, F. Been, A. Celma, S. Castiglioni, Perspectives and challenges associated with  
647 the determination of new psychoactive substances in urine and wastewater—A tutorial, *Anal Chim*  
648 *Acta* 1145 (2021) 132-147.

649 [23] J.N. Dodds, Z.R. Hopkins, D.R.U. Knappe, E.S. Baker, Rapid Characterization of Per- and  
650 Polyfluoroalkyl Substances (PFAS) by Ion Mobility Spectrometry-Mass Spectrometry (IMS-MS), *Anal*  
651 *Chem* 92(6) (2020) 4427-4435.

652 [24] S. Gosciny, M. McCullagh, J. Far, E. De Pauw, G. Eppe, Towards the use of ion mobility mass  
653 spectrometry derived collision cross section as a screening approach for unambiguous identification  
654 of targeted pesticides in food, *Rapid Commun Mass Spectrom* 33 (2019) 34-48.

655 [25] E. Canellas, P. Vera, C. Nerin, Ion mobility quadrupole time-of-flight mass spectrometry for the  
656 identification of non-intentionally added substances in UV varnishes applied on food contact  
657 materials. A safety by design study, *Talanta* 205 (2019) 120103.

658 [26] K.M. Hines, J. Herron, L. Xu, Assessment of altered lipid homeostasis by HILIC-ion mobility-mass  
659 spectrometry-based lipidomics, *J. Lipid Res.* 58(4) (2017) 809-819.

660 [27] X. Zheng, N.A. Aly, Y. Zhou, K.T. Dupuis, A. Bilbao, V.L. Paurus, D.J. Orton, R. Wilson, S.H. Payne,  
661 R.D. Smith, A structural examination and collision cross section database for over 500 metabolites  
662 and xenobiotics using drift tube ion mobility spectrometry, *Chemical science* 8(11) (2017) 7724-  
663 7736.

664 [28] M. Hernandez-Mesa, B. Le Bizec, F. Monteau, A.M. Garcia-Campana, G. Dervilly-Pinel, Collision  
665 Cross Section (CCS) Database: An Additional Measure to Characterize Steroids, *Anal Chem* 90(7)  
666 (2018) 4616-4625.

667 [29] D.H. Ross, J.H. Cho, L. Xu, Breaking down structural diversity for comprehensive prediction of  
668 ion-neutral collision cross sections, *Anal Chem* 92(6) (2020) 4548-4557.

669 [30] J.A. Picache, B.S. Rose, A. Balinski, K.L. Leaptrot, S.D. Sherrod, J.C. May, J.A. McLean, Collision  
670 cross section compendium to annotate and predict multi-omic compound identities, *Chem Sci* 10(4)  
671 (2019) 983-993.

672 [31] Z. Zhou, X. Shen, J. Tu, Z.J. Zhu, Large-Scale Prediction of Collision Cross-Section Values for  
673 Metabolites in Ion Mobility-Mass Spectrometry, *Anal Chem* 88(22) (2016) 11084-11091.

674 [32] Z. Zhou, M. Luo, X. Chen, Y. Yin, X. Xiong, R. Wang, Z.J. Zhu, Ion mobility collision cross-section  
675 atlas for known and unknown metabolite annotation in untargeted metabolomics, *Nat Commun*  
676 11(1) (2020) 4334.

677 [33] Z. Zhou, J. Tu, X. Xiong, X. Shen, Z.J. Zhu, LipidCCS: Prediction of Collision Cross-Section Values  
678 for Lipids with High Precision To Support Ion Mobility-Mass Spectrometry-Based Lipidomics, *Anal*  
679 *Chem* 89(17) (2017) 9559-9566.

680 [34] C.B. Mollerup, M. Mardal, P.W. Dalsgaard, K. Linnet, L.P. Barron, Prediction of collision cross  
681 section and retention time for broad scope screening in gradient reversed-phase liquid  
682 chromatography-ion mobility-high resolution accurate mass spectrometry, *J. of Chrom A* 1542  
683 (2018) 82-88.

684 [35] S.M. Colby, D.G. Thomas, J.R. Nunez, D.J. Baxter, K.R. Glaesemann, J.M. Brown, M.A. Pirrung, N.  
685 Govind, J.G. Teeguarden, T.O. Metz, R.S. Renslow, ISiCLE: A Quantum Chemistry Pipeline for  
686 Establishing in Silico Collision Cross Section Libraries, *Anal Chem* 91(7) (2019) 4346-4356.

687 [36] L. Bijlsma, R. Bade, A. Celma, L. Mullin, G. Cleland, S. Stead, F. Hernandez, J.V. Sancho,  
688 Prediction of Collision Cross-Section Values for Small Molecules: Application to Pesticide Residue  
689 Analysis, *Anal Chem* 89(12) (2017) 6583-6589.

690 [37] L. Bijlsma, M.H. Berntssen, S. Merel, A refined nontarget workflow for the investigation of  
691 metabolites through the prioritization by in silico prediction tools, *Anal Chem* 91(9) (2019) 6321-  
692 6328.

693 [38] D. Fabregat-Safont, M. Ibáñez, L. Bijlsma, F. Hernández, A.V. Waichman, R. de Oliveira, A. Rico,  
694 Wide-scope screening of pharmaceuticals, illicit drugs and their metabolites in the Amazon River,  
695 *Water Research* 200 (2021) 117251.

696 [39] T.J. Causon, S. Hann, Uncertainty Estimations for Collision Cross Section Determination via  
697 Uniform Field Drift Tube-Ion Mobility-Mass Spectrometry, *J Am Soc Mass Spectrom* 31(10) (2020)  
698 2102-2110.

699 [40] L. Righetti, N. Dreolin, A. Celma, M. McCullagh, G. Barknowitz, J.V. Sancho, C. Dall'Asta,  
700 Travelling Wave Ion Mobility-Derived Collision Cross Section for Mycotoxins: Investigating  
701 Interlaboratory and Interplatform Reproducibility, *J Agric Food Chem* 68(39) (2020) 10937-10943.

702 [41] A. Celma, R. Bade, J.V. Sancho, F. Hernández, M. Humpries, L. Bijlsma, Prediction of Retention  
703 Time and Collision Cross Section (CCSH<sup>+</sup>, CCSI<sup>-</sup> and CCSNa<sup>+</sup>) of emerging contaminants using  
704 Multiple Adaptive Regression Splines. Preprint at <https://doi.org/10.21203/rs.3.rs-1249834/v1>. Tool  
705 available at: [https://datascience-adelaideuniversity.shinyapps.io/Predicting\\_RT\\_and\\_CCS/](https://datascience-adelaideuniversity.shinyapps.io/Predicting_RT_and_CCS/), (2022).

706 [42] I. Campuzano, M.F. Bush, C.V. Robinson, C. Beaumont, K. Richardson, H. Kim, H.I. Kim, Structural  
707 characterization of drug-like compounds by ion mobility mass spectrometry: comparison of  
708 theoretical and experimentally derived nitrogen collision cross sections, *Anal Chem* 84(2) (2012)  
709 1026-1033.

710 [43] M.F. Bush, I.D. Campuzano, C.V. Robinson, Ion mobility mass spectrometry of peptide ions:  
711 effects of drift gas and calibration strategies, *Anal Chem* 84(16) (2012) 7124-7130.

712 [44] I. Sushko, S. Novotarskyi, R. Körner, A.K. Pandey, M. Rupp, W. Teetz, S. Brandmaier, A.  
713 Abdelaziz, V.V. Prokopenko, V.Y. Tanchuk, Online chemical modeling environment (OCHEM): web  
714 platform for data storage, model development and publishing of chemical information, *J. Comput*  
715 *Aid Mol Des* 25(6) (2011) 533-554.

716 [45] P.L. Plante, E. Francovic-Fontaine, J.C. May, J.A. McLean, E.S. Baker, F. Laviolette, M. Marchand,  
717 J. Corbeil, Predicting Ion Mobility Collision Cross-Sections Using a Deep Neural Network: DeepCCS,  
718 *Anal Chem* 91(8) (2019) 5191-5199.

719 [46] K.M. Hines, J.C. May, J.A. McLean, L. Xu, Evaluation of collision cross section calibrants for  
720 structural analysis of lipids by traveling wave ion mobility-mass spectrometry, *Analytical chemistry*  
721 88(14) (2016) 7329-7336.  
722 [47] M.L. Feuerstein, M. Hernández-Mesa, Y. Valadbeigi, B. Le Bizec, S. Hann, G. Dervilly, T. Causon,  
723 Critical evaluation of the role of external calibration strategies for IM-MS, *Analytical and*  
724 *Bioanalytical Chemistry* (2022) 1-11.  
725